JOURNAL OF
MOLECULAR
CATALYSIS
A: CHEMICAL

In situ UV–Vis diffuse reflectance spectroscopy — *on line* activity measurements of supported chromium oxide catalysts: relating isobutane dehydrogenation activity with Cr-speciation via experimental design

Bert M. Weckhuysen [a,*], An A. Verberckmoes [a], Jan Debaere [a], Kristine Ooms [b], Ivan Langhans [b], Robert A. Schoonheydt [a]

[a] *Centrum voor Oppervlaktechemie en Katalyse, Departement Interfasechemie, K.U. Leuven, Kardinaal Mercierlaan 92, 3001 Heverlee, Belgium*
[b] *CQ Consultancy, Innovatie- en Incubatiecentrum, K.U. Leuven, Kapeldreef 60, 3001 Heverlee, Belgium*

Abstract

The dehydrogenation of isobutane over supported chromium oxide catalysts was studied by a combination of in situ UV–Vis diffuse reflectance spectroscopy and *on line* GC analysis. A well-defined set of experiments, based on an experimental design, was carried out to develop mathematical models, which quantitatively relate Cr-speciation and dehydrogenation activity with reaction temperature and time, support composition, gas composition and Cr loading. It will be shown that: (1) the dehydrogenation activity is proportional with the amount of in situ measured surface $Cr^{2+/3+}$, and maximum for a 7.5 wt.% Cr/Al_2O_3 catalyst operating at 500°C in 2% isobutane in N_2; and (2) Cr^{3+}-sites are more active in alkane dehydrogenation than Cr^{2+}-sites. This paper is the first example of the use of experimental design for deriving structure–activity relationships in the field of heterogeneous catalysis. © 2000 Elsevier Science B.V. All rights reserved.

1. Introduction

The catalytic dehydrogenation of propane and isobutane over supported chromium oxide catalysts has a considerable industrial impact because it represents a route to obtain alkenes from feedstock of low-cost saturated hydrocarbons [1,2]. In particular, isobutane dehydrogena-tion is nowadays important because the tradi-tional sources of isobutane; i.e., steam cracking and fluid catalytic cracking, are already heavily used, and the availability of isobutane has be-come a bottle-neck in the expansion of the MTBE and ETBE market.

Most characterization studies on supported chromium oxide catalysts describe the catalyst structure under conditions often far away from real catalytic ones [3]. As a consequence, only a limited amount of information is known about

---

* Corresponding author. Fax: +32-16-32-19-98; E-mail: bert.weckhuysen@agr.kuleuven.ac.be

the oxidation state and coordination environment of the active dehydrogenation site [4–8]. Therefore, research must be directed towards the catalytic characterization under in situ conditions [9–11].

In this work, a novel method has been developed for deriving quantitative structure–activity relationships by using the technique of experimental design. It is important to stress that this technique has been successfully introduced in the field of drugs and pharmaceuticals design [12–14], but — to our best knowledge — not in the field of heterogeneous catalysis. The goal of this paper is to explore its possibilities and limitations for studying heterogeneous catalysts. We have chosen the dehydrogenation of isobutane over supported chromium oxide catalysts as model reaction because we have studied this system in great detail in the past. The used spectroscopic technique is UV–Vis diffuse reflectance spectroscopy, which allows to monitor in situ Cr^{6+}, Cr^{3+} and Cr^{2+} [9–11,15,16]. The developed method involves a three-pronged approach. In a first step, the number of required experiments was optimized by using an experimental design, and five factors were selected to describe the dehydrogenation process. Secondly, both Cr-speciation and dehydrogenation activity were measured by in situ diffuse reflectance spectroscopy and *on line* GC analysis, respectively. In a final step, a mathematical or statistical model for the optimization of isobutane dehydrogenation was derived. The obtained conditions are compared with those used in chemical industry.

2. Experimental

2.1. Catalyst preparation

2.1.1. Preparation of supports

SiO_2 was prepared by mixing 2 vol. parts H_2O at pH 2 (adding HCl) and 1 vol. part tetraethyl orthosilicate (TEOS) during 5 h at room temperature. The mixture was titrated under stirring to pH 6 with a NH_4OH solution of pH 9.5. After 16 h of gelation, the gel was dried at 130°C for 72 h and calcined at 250 and 550°C for 3 and 16 h, respectively. The so-obtained cake was crushed. $SiO_2 \cdot Al_2O_3$ with 60 wt.% SiO_2 was prepared following a modified method of Chen et al. [17]. Appropriate amounts of TEOS and aluminum triisopropoxide were mixed in 128 ml of ethanol during 30 min at room temperature. After adding 35 ml of 1 M HCl, the hydrolysis started and the solution was mixed for 1 h. The gel was dried at 60 and 100°C for 8 h, and calcined at 550°C for 16 h. The $SiO_2 \cdot Al_2O_3$ was crushed. Al_2O_3 was prepared by drying an ethanol solution of aluminumtriisopropoxide at 60 and 100°C for 8 h. The dried solid was further calcined at 550°C for 16 h. TiO_2 (P25) and ZrO_2 (16.052.40) were obtained from Degussa and Merck, respectively. The characteristics of the supports were measured by dynamic N_2 adsorption on an Omnisorp 100 (Coulter), after pretreatment in vacuum at 200°C for 8 h, while their isoelectric points (IEP) were determined via charge titration [18]. The characteristics of the supports are given in Table 1.

2.1.2. Preparation of catalysts

The supported chromium oxide catalysts were prepared by the incipient-wetness method with chromium(VI)oxide (CrO_3). The catalysts were dried at 50°C for 8 h and granulated. The size fraction between 0.2 and 0.5 mm were used for in situ DRS measurements. The Cr loadings of the catalysts were 0.1, 0.5, 0.55, 4, 7.5 and 8 wt.%. Taking into account (1) the surface areas of the used supports (Table 1); and (2) that

Table 1
Characteristics of the supports

Support	Surface area (m^2/g)	IEP
SiO_2	450	2
$SiO_2 \cdot Al_2O_3$	260	5
Al_2O_3	360	8
TiO_2	55	5
ZrO_2	39	5

monolayer coverage is only reached at about 4 Cr/nm^2 [1], one can conclude that the Cr-based catalysts under study (with the exception of 4 wt.% $/ZrO_2$) are below monolayer coverage and predominantly contain surface Cr-species.

2.2. In situ diffuse reflectance spectroscopy — on line GC analysis

In situ diffuse reflectance spectra were taken on a Varian Cary 5 UV–Vis–NIR spectrophotometer equipped with a specially designed Praying Mantis diffuse reflection attachment (DRA) of Harrick. A schematic drawing of this cell is given in Fig. 1 and the technical details of the cell are given in recent papers [15,16]. The white reflectance standard $BaSO_4$ (Kodak) was used to take a baseline at 25°C in the Praying Mantis cell. The thickness of the catalyst bed was 3 mm, and the amount of the catalyst used was around 50 mg. The catalyst was first treated in oxygen in the in situ cell at 550°C for 1 h, and then cooled in He to the reaction temperature. The reaction conditions applied to the catalyst sample were chosen according to an experimental design, which is outlined below. The measured in situ DRS spectra were processed with several software packages: (1) Grams/386 (Galactic Industries); (2) SIMPLISMA (developed by Willem Windig, Eastman Kodak); and (3) PCA of the Chemometric toolbox for Matlab (The Math Works).

Details about these packages can be found in Refs. [19–21]. *On line* gas chromatography analysis was done with a HP 5830 GC instrument equipped with a FID detector, 6-way valve inlet system, and a packed column filled with *n*-octane/porasil-C (100–120 mesh, Durapack, Applied Science Laboratories).

3. Experimental design

Five factors ($\mathbf{X}$'s) were selected to quantitatively describe the differences in dehydrogenation activity (y) and Cr-speciation (z) between supported chromium oxide catalysts. This is illustrated in Fig. 1. The factors under study were: $\mathbf{X}_1$, the support composition, characterized by its IEP; $\mathbf{X}_2$, the Cr loading (wt.% Cr); $\mathbf{X}_3$, the gas composition, characterized by the percentage of isobutane in N_2; $\mathbf{X}_4$, the reaction temperature and $\mathbf{X}_5$, the reaction time. The limits of each of these factors were as follows: $\mathbf{X}_1$: 2 and 8; $\mathbf{X}_2$: 0.5 and 7.5 wt.% Cr; $\mathbf{X}_3$: 2 and 18% isobutane in He; $\mathbf{X}_4$: 350 and 500°C and $\mathbf{X}_5$: 10 and 50 min.

The selection of these five factors was based on our preliminary work of *n*-butane dehydrogenation over supported chromium oxide catalysts [11], and on literature results [1–3]. Indeed, it was previously found that the alkane dehydrogenation activity was related with the Cr loading, the support composition, gas com-
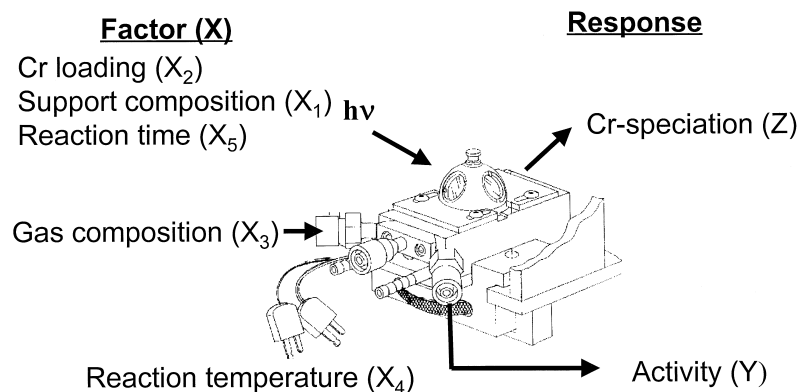

Fig. 1. Schematic drawing of the in situ DRS cell, and the experimental design under study.

position and the reaction time and temperature. It is important to stress that other factors such as the possible formation of solid solutions are equally important. The latter is especially true for catalyst recycling; however, long-term deactivation via the formation of a solid solution (e.g., $Cr_x Al_{2-x} O_3$) will not be the subject of this paper, and is therefore excluded. Therefore, we have limited ourselves to a detailed study of the influence of the five factors on both the dehydrogenation activity and Cr speciation.

The values of each of the above-described factors can be easily changed between (experimental) limits. The most difficult point here is to use an appropriate parameter to describe the support. However, as was shown in previous publications [3,19,22–24], it is especially the

chemical composition ($SiO_2:Al_2O_3$ ratio) of the support which determines — via its chemical hardness/softness, solid-state chemistry and hydroxyl chemistry — the dispersion, coordination environment, oxidation state and polymerization degree of Cr species. We have chosen the IEP as a parameter to describe the support composition because the IEP is directly related with the $SiO_2:Al_2O_3$ ratio of the supports (Table 1): a high IEP value corresponds with a low $SiO_2:Al_2O_3$ ratio for $SiO_2 \cdot Al_2O_3$ supports.

The methodology, which was followed in this work, is a well-established approach known as Response Surface Modelling (RSM) [25]. In RSM the usually nonlinear multivariate relation between the characteristics under study y or z

Table 2

Five-level circumscribed central composite experimental design generated by the MODDE program for optimizing isobutane dehydrogenation over supported chromium oxide catalysts

Experiment number	Experiment name	Run order	Factor X_1	Factor X_2	Factor X_3	Factor X_4	Factor X_5	Response y	Response z
1	N01	12	2	0.5	2	350	50	0.070	0.090
2	N02	26	8	0.5	2	350	10	0.63	0.17
3	N03	8	2	7.5	2	350	10	4.30	1.26
4	N04	9	8	7.5	2	350	50	0.88	2.55
5	N05	4	2	0.5	18	350	10	0.44	0.086
6	N06	27	8	0.5	18	350	50	0.090	0.23
7	N07	18	2	7.5	18	350	50	0.33	1.29
8	N08	2	8	7.5	18	350	10	1.26	2.52
9	N09	13	2	0.5	2	500	10	1.71	0.24
10	N10	10	8	0.5	2	500	50	0.24	0.65
11	N11	19	2	7.5	2	500	50	1.18	3.57
12	N12	21	8	7.5	2	500	10	5.18	7.23
13	N13	17	2	0.5	18	500	50	0.090	0.25
14	N14	5	8	0.5	18	500	10	1.40	0.65
15	N15	3	2	7.5	18	500	10	1.09	3.66
16	N16	11	8	7.5	18	500	50	1.48	7.15
17	N17	6	2	4	10	425	30	0.040	0.78
18	N18	1	8	4	10	425	30	0.20	2.35
19	N19	23	5	0.1	10	425	30	0.05	0.080
20	N20	22	5	8	10	425	30	0.11	0.54
21	N21	24	5	4	1	425	30	1.77	1.16
22	N22	14	5	4	19	425	30	0.090	1.25
23	N23	7	5	4	10	300	30	0.12	0.65
24	N24	15	5	4	10	550	30	0.73	5.80
25	N25	20	5	4	10	425	5	1.75	1.10
26	N26	16	5	4	10	425	55	0.060	1.25
27	N27	25	5	4	10	425	30	0.090	1.26
28	N28	28	5	4	10	425	30	0.090	1.25
29	N29	29	5	4	10	350	30	0.24	0.48
30	N30	30	5	0.55	10	350	30	0.070	0.13

(the responses) and factors $\mathbf{X}_i$ is being modelled by means of a low-order polynomial. This is usually a second-order polynomial:

$$y = \beta_0 + \sum_i^5 \beta_i X_i + \sum_{i \neq j} \Sigma \beta_{ij} X_i X_j + \sum_i^5 \beta_{ii} X_i^2 \tag{1}$$

with y, the response; β_0, a constant; β_i, the model coefficients for each factor; β_{ij}, the model coefficients of the interaction terms; β_{ii}, the model coefficients of the quadratic terms; and $\mathbf{X}_i$, the factor i. This is in fact nothing else than a multivariable second-order Taylor approximation. To quantify this multivariable relation (or better: its polynomial representation) in an optimal way, an approach called experimental design is needed [20,25]. The optimal design for this particular catalysis problem was a central composite design. This is essentially a five-level design where some points (the ''star-points'') exceed the specified factor limits by a chosen amount, and thus allows to check whether the second-order approximation was sufficient or not.

The generated spreadsheet in this study, which was generated by MODDE for Windows 3.0 (Umetri) [25] and containing information about the set of 30 experiments (i.e., experiment name, run order and experimental conditions for the different factors), is summarized in Table 2. However, this experimental design is different from a standard central composite design in a number of ways.

–One of the variables, namely $\mathbf{X}_1$, could only take three values, which means that it will not be possible to check whether the second-order approximation of the underlying relation is adequate or not. The reason is, of course, that there are no $SiO_2 \cdot Al_2O_3$ supports available with an IEP lower than 2 and higher than 8.

–The star-points for the factors $\mathbf{X}_2$–$\mathbf{X}_4$ were put only slightly outside the initially specified limits.

–The number of centerpoints (which are the experiments repeated during the course of the experimental design) was reduced to two (experiments N27 and N28 in Table 2).

–Two extra points (experiments N29 and N30 in Table 2) consisted of two different supports (i.e., TiO_2 and ZrO_2) having the same IEP as the $SiO_2 \cdot Al_2O_3$s (5) were also introduced. These experiments can be considered as measures for testing how well the representation of the supports by their IEP holds.

4. Results

4.1. Quantitative relationship between the dehydrogenation activity and the reaction time and temperature, the gas composition, the support composition and the Cr-loading

By measuring the catalytic activity for the set of 30 experiments by *on line* GC analysis, one can obtain the response values y in Table 2. It is important to stress here that the selectivities towards isobutane were always very high, and reaches a maximum at around 90–95%. Therefore, the catalytic conversions as measured by *on line* GC analysis in the in situ cell are a good measure of the catalytic performances of the supported chromium oxide catalysts. The influence of the different design variables or factors $\mathbf{X}_i$ (the reaction time and temperature, the gas composition, the support composition and the Cr-loading) on the response y (dehydrogenation activity, expressed as catalytic conversion) could be determined by applying a statistical model based on multiple linear regression (MLR). This analysis, which is extensively described in the literature, was done with the software package MODDE [25]. The approach essentially consists of the following steps:

–Fitting an initial model using MLR;
–Checking the transformations of the response y (a Box–Cox analysis);

Table 3

Unscaled coefficients β for the model relating the dehydrogenation activity and the reaction time and temperature, the gas composition, the support composition and the Cr-loading

Model coefficient β	Unscaled value
β_1	-0.195
β_2	0.121
β_3	-0.132
β_4	$-9.540 \cdot 10^{-4}$
β_5	-0.0610
β_{33}	$4.941 \cdot 10^{-3}$
β_{55}	$5.875 \cdot 10^{-4}$
β_{14}	$5.137 \cdot 10^{-4}$
β_{23}	$-4.480 \cdot 10^{-3}$
β_{35}	$8.008 \cdot 10^{-4}$
β_0	2.248

–Validating the fitted model using an Analysis Of Variance (ANOVA) (see Appendix B) and residual analysis;
–Visualizing the relations between response and factors (response surface plots).

The result of such chemometrical analysis is shown in Table 3, and 11 model coefficients are obtained. The relation between the catalytic activity, expressed as $y^{1/2}$, and the factors of the experimental design is given in Eq. (2):

$$
\begin{aligned}
y^{\frac{1}{2}}(\%) = {} & 2.248 - 0.195\,X_1 + 0.121\,X_2 \\
& - 0.132\,X_3 - 9.540 \cdot 10^{-4} X_4 \\
& - 0.0610\,X_5 + 4.941 \cdot 10^{-3} X_3^2 \\
& + 5.875 \cdot 10^{-4} X_5^2 + 5.137 \cdot 10^{-4} X_1 X_4 \\
& - 4.480 \cdot 10^{-3} X_2 X_3 \\
& - 8.008 \cdot 10^{-4} X_3 X_5 \qquad (2)
\end{aligned}
$$

This model is statistically significant, and results in a very good R^2 value of 0.91 (see Appendix A) and a RMSE of 0.2 (with RMSE, the root mean square error; i.e., the standard deviation of the differences between fitted and measured response values). The quality of the fit, visualized in Fig. 2, is quite reasonable, but not perfect because there seems to be some minor higher-order effects operative. However,

Eq. (2) allows to calculate the conditions in order to maximize the dehydrogenation activity over supported chromium oxide catalysts. The following conditions were obtained: $\mathbf{X}_1 = 8$; $\mathbf{X}_2 = 7.5$; $\mathbf{X}_3 = 2$; $\mathbf{X}_4 = 500$ and $\mathbf{X}_5 = 10$. Thus, a predicted maximum conversion of 5.58% is obtained after 10 min for a 7.5 wt.% Cr/Al_2O_3 catalyst at 500°C with a mixture of 2% isobutane in N_2, which is close to the experimental value of 5.18% (Experiment N12 in Table 2 and Fig. 2).

In order to visualize Eq. (2), one can make conversion surface plots, as illustrated in Fig. 3. For example, Fig. 3A predicts the catalytic activity after 30 min for a $Cr/SiO_2 \cdot Al_2O_3$ catalyst at 425°C as a function of the amount of isobutane in N_2 and as a function of the Cr loading. It is clear that the dehydrogenation activity gradually increases with increasing Cr loading and decreasing amount of isobutane in N_2. The influence of the reaction time and the Cr loading on the predicted dehydrogenation activity of a $Cr/SiO_2 \cdot Al_2O_3$ catalyst at 425°C is illustrated in Fig. 3B. It shows a gradual decrease in activity with increasing reaction time. The combined effect of the IEP of the support of the support and the reaction temperature on the catalytic activity is given in Fig. 3C. One can notice that at high reaction temperatures the dehydrogenation activity increases with increasing IEP; i.e., with an increasing amount of Al_2O_3 in the support.

Finally, it is important to note that the IEP of the support seems to be a good measure to differentiate between the different support compositions. This is clear from the results of experiments N29 and N30 (Table 2). Although in both experiments use has been made of two different supports; i.e., ZrO_2 and TiO_2, no significant differences were observed with a $Cr/SiO_2 \cdot Al_2O_3$ (60 wt.% SiO_2) catalyst, which has an identical IEP. Thus, experiments N29 and N30 are not detected as outliers within the frame of our experimental design, and the IEP is a good measure to differentiate between the different supports.
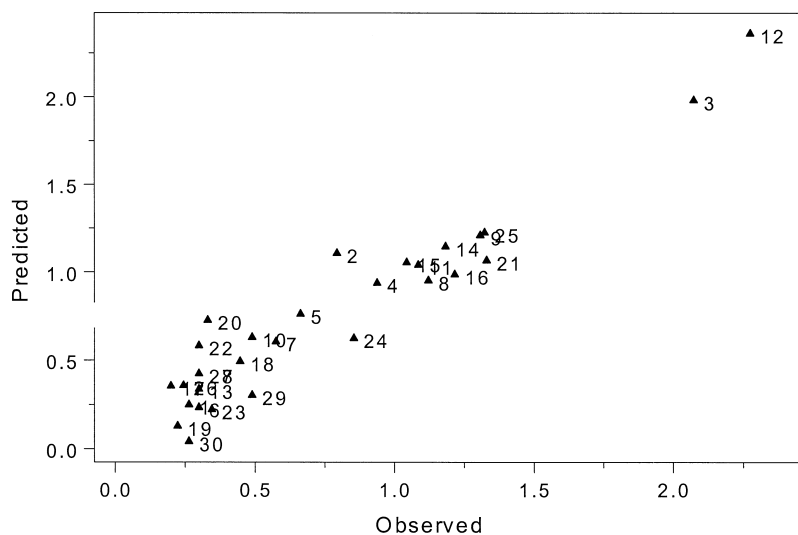
Fig. 2. Predicted vs. observed values of $y^{1/2}$ for the statistical model relating the catalytic activity with factors (model parameters are given in Table 3).

4.2. Quantitative relationship between the Cr-speciation and the reaction temperature, the support composition and the Cr-loading

4.2.1. Determination of Cr-speciation via in situ DRS spectroscopy

In situ diffuse reflectance spectra were monitored between 200 and 800 nm as a function of time for each experiment of Table 2. The scan time was 1 min, and 60 different spectra were recorded during 1 h. An example of a set of in situ diffuse reflectance spectra is given in Fig. 4 for experiment N01 and N06. N01 is an experiment with a 0.5 wt.% Cr/SiO_2 catalyst treated at 350°C in 2% isobutane, and the corresponding DRS spectra are given in Fig. 4A. Fig. 4A shows a gradual decrease of absorption maxima around 360 and 450 nm with increasing reaction time at the expense of a new weak band with an absorption maximum at around 625 nm. The insert of Fig. 4A illustrates the presence of an isobestic point, suggesting the presence of two different Cr-species. By applying principal component analysis (PCA) — a common chemometric technique, which is briefly explained in Appendix C — to the set of spectra of Fig. 4A, two principal components were obtained. An-

other chemometrical technique to unravel a series of spectra is SIMPLISMA (Appendix D). This technique does not only determine the number of pure component spectra in the experimental diffuse reflectance spectra, but also delivers each of the pure component spectra, together with their intensity profile (see Appendix D). In a previous paper, we have shown the possibilities and limitations of this method in the unravelling of DRS spectra of supported chromium oxide catalysts in great detail [19]. The results of this approach are shown in Fig. 5A for experiment N01. The first pure component has two absorption bands/shoulders at 460 and 373 nm, which can be assigned to the spin-forbidden $1t_1 \rightarrow 2e$ transition and the spin-allowed $1t_1 \rightarrow 2e$ transition of dichromate, respectively [3,19,22–24]. The other pure component spectrum has absorption maxima around 632 nm and 435 nm. The broad absorption band, extending to higher wavelength, is a superposition of pseudo-tetrahedral Cr^{2+} (the $^5T_2 \rightarrow {}^5E$ transition) and pseudo-octahedral $Cr^{2+/3+}$ ($^5E_g \rightarrow {}^5T_{2g}$ transition/$^4A_{2g} \rightarrow {}^4T_{2g}$ transition) [3]. The 435 nm band must be due to the $^4A_{2g} \rightarrow {}^4T_{1g}(^4F)$ transition of (pseudo-) octahedral Cr^{3+}, whereas $^4A_{2g} \rightarrow {}^4T_{1g}(^4P)$ transition is
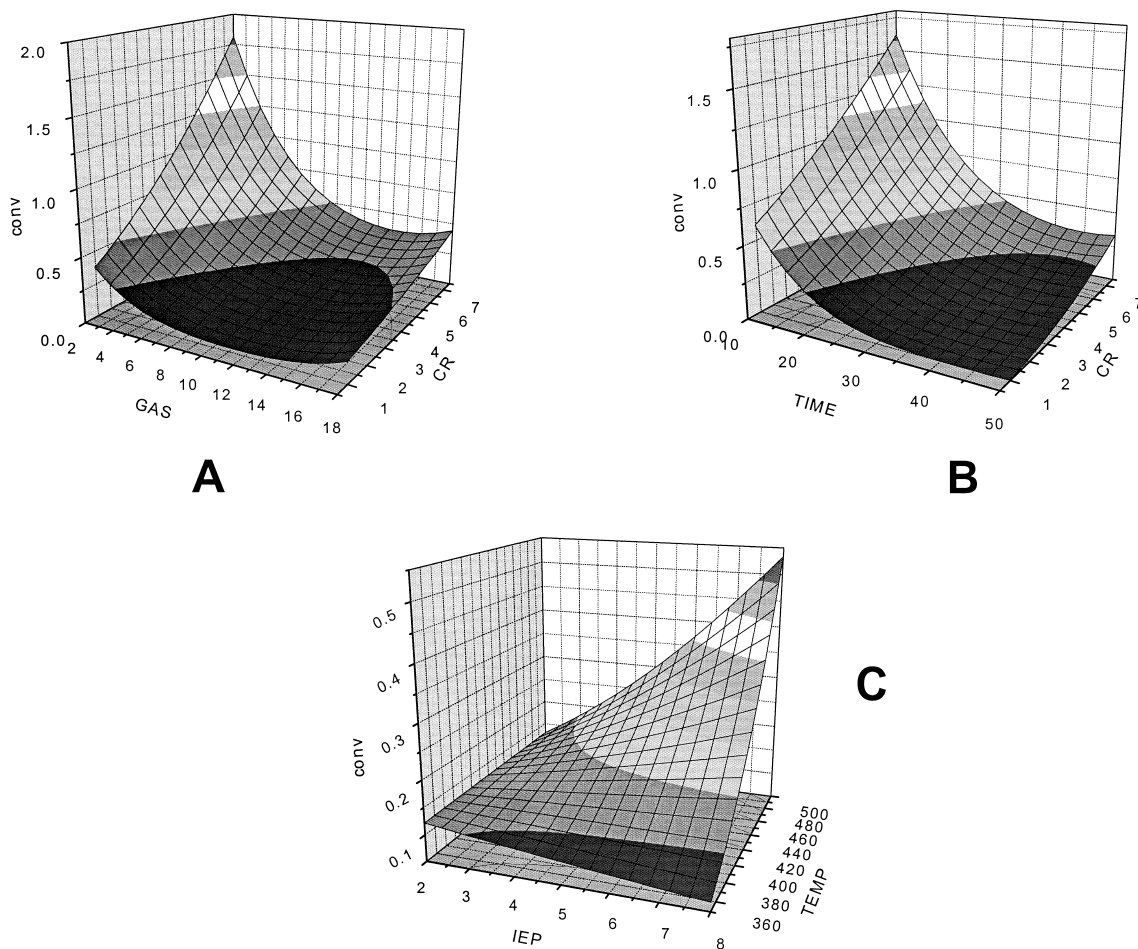
Fig. 3. (A) Conversion surface plot of the gas composition and Cr-loading (the reaction temperature, IEP of the support and the reaction time are 425°C, 5 and 10 min, respectively). (B) Conversion surface plot of the reaction time and Cr loading (the IEP, gas composition and reaction temperature are 5, 10% isobutane and 425°C, respectively). (C) Conversion surface plot of the IEP of the support and the reaction temperature (the Cr loading, gas composition and reaction time are 4 wt.%, 10% isobutane and 30 min, respectively).

only visible as a shoulder at around 330 nm [3]. Summarizing, the first pure component spectrum is typical for Cr^{6+}, whereas the second pure component spectrum is indicative for the presence of $Cr^{2+/3+}$ [3,19,22–24].

The same procedure can be applied for experiment N06, which is about a 0.5 wt.% Cr/Al_2O_3 catalyst treated in 18% isobutane in N_2 at 350°C. Fig. 4B shows a gradual decrease of the intensity of the absorption maximum around 380 nm with increasing reaction time at the expense of a new weak band with an absorption maximum at around 590 nm. By applying PCA two principal

components were obtained, and the results of the SIMPLISMA analysis are given in Fig. 5B. Two pure component spectra were obtained. The first pure component has a clear absorption maximum at around 389 nm, and is assigned to the spin-allowed $1t_1 \rightarrow 2e$ transition of chromate [3,19,22–24]. The second pure component has a broad absorption maximum starting at around 450 nm to higher nm, which encompasses predominantly the two characteristic transitions of (pseudo-) octahedral Cr^{3+}, and is also indicative for the presence of small amounts of (pseudo-) octahedral Cr^{2+}. The shoulder at
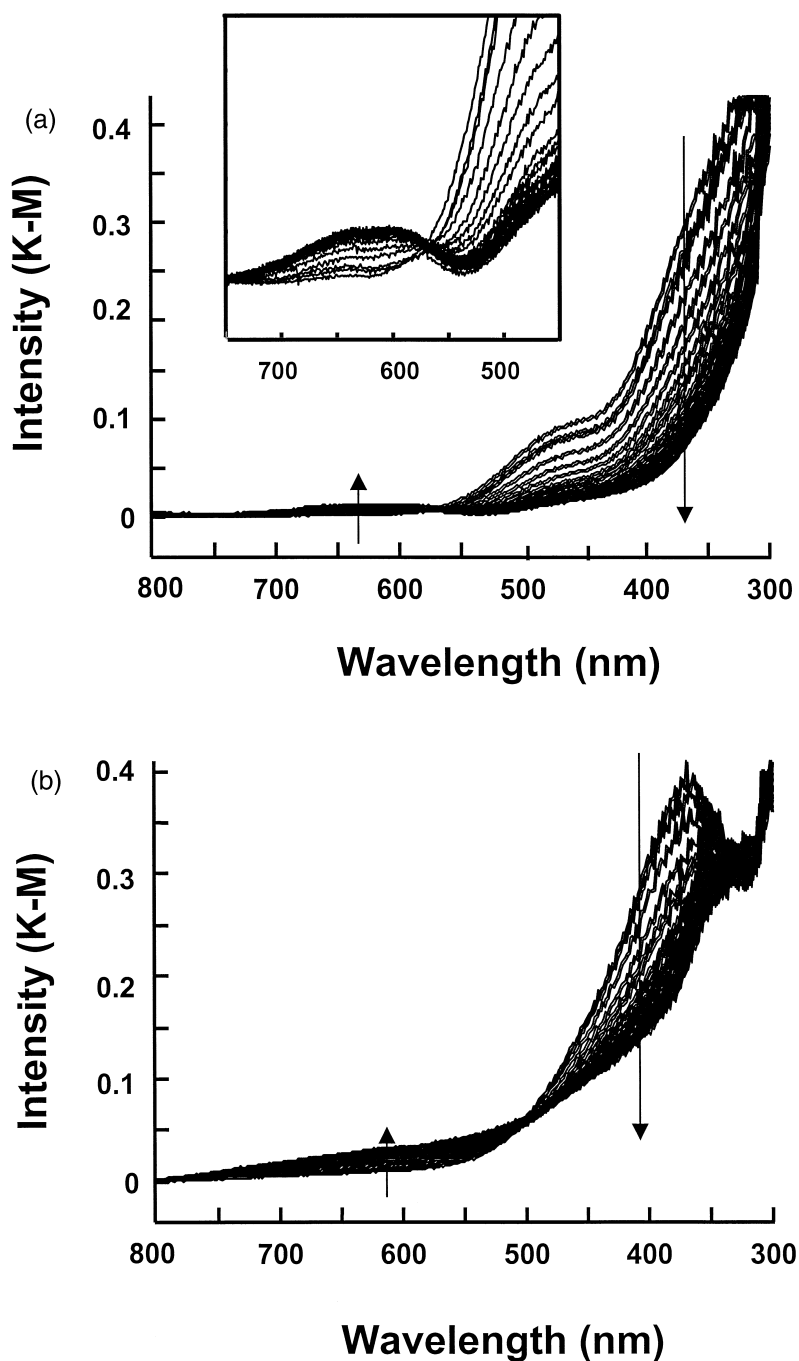
Fig. 4. (A) In situ UV–Vis diffuse reflectance spectra of 0.5 wt.% Cr/SiO_2 catalyst treated at 350°C in 2% isobutane in N_2 as a function of time (Experiment N01). (B) In situ UV–Vis diffuse reflectance spectra of 0.5 wt.% Cr/Al_2O_3 catalyst treated at 350°C in 2% isobutane in N_2 as a function of time (Experiment N06).

around 330 nm is assigned to the $^4A_{2g} \rightarrow ^4T_{1g}$ (^4P) transition of (pseudo-) octahedral Cr^{3+} [3,19,22–24].

By applying both PCA and SIMPLISMA techniques to all the series of in situ diffuse reflectance spectra of Table 2, we were able to

Fig. 5. (A) Pure component spectra, and their corresponding intensity profiles, of the in situ diffuse reflectance spectra of Fig. 4A (Experiment N01). The intensity profiles have been obtained by plotting the band intensities at 373 nm (1st pure component) and 632 nm (2nd pure component) as a function of time. (B) Pure component spectra, and their corresponding intensity profiles, of the in situ diffuse reflectance spectra of Fig. 4B (Experiment N06). The intensity profiles have been obtained by plotting the band intensities at 389 nm (1st pure component) and 570 nm (2nd pure component) as a function of time.

determine that in all cases: (1) Two principal components are sufficient to explain the variance of the overlapping in situ diffuse reflectance spectra within one set of experiments; (2) The absorption maxima of the pure component spectra extracted by the SIMPLISMA technique differ from one support to another. In-

deed, as discussed above, the absorption maxima of reduced Cr is around 570 nm for Cr/Al_2O_3 catalysts, and around 630 nm for Cr/SiO_2 catalysts. These discrepancies are due to differences in Cr-speciation; i.e., mainly Cr^{3+} on Al_2O_3, and Cr^{2+} mainly on SiO_2 supports [3], and these spectroscopic differences have been discussed in detail in previous papers [9–11,15,16,22–24]; (3) The noise level of both the in situ diffuse reflectance spectra and the corresponding pure component spectra increases with increasing Cr-loading and reaction time. The former is due to a decreasing amount of reflected light from the samples, while the latter is related with coke formation.

In order to develop a relevant model to relate the Cr-speciation with the reaction time and temperature, the gas composition, the support composition and the Cr-loading, one has to define the response factor z. We have selected as response factor z the Kubelka–Munk (K–M) intensity of the band typical for reduced $Cr^{2+/3+}$. The band maximum of reduced $Cr^{2+/3+}$ is located between 570 and 630 nm, its exact value depending on the support composition (vide supra). This response factor is further denoted as $K–M(Cr^{3+/2+})$, and by extracting the $K–M(Cr^{3+/2+})$ values from the intensity profiles of the pure component spectra, we were able to complete Table 2. The selection of the $K–M(Cr^{3+/2+})$ value as response factor deserves some additional comments. First of all, it is sufficient to include the $K–M(Cr^{3+/2+})$ values in our model because the K–M values of the Cr^{6+}-species are directly related with those of reduced $Cr^{3+/2+}$. Secondly, the $K–M(Cr^{3+/2+})$ values are proportional with the concentration of $Cr^{3+/2+}$ according to Eq. (3):

$$K–M(Cr^{3+/2+})$$

$$= \frac{(1 - R_\infty)^2}{2R_\infty} = \frac{K}{S} = k^* C(Cr^{3+/2+}) \qquad (3)$$

with $K–M(Cr^{3+/2+})$, the Kubelka–Munk intensity; R_∞, the diffuse reflectance of the catalyst;

Table 4
Unscaled coefficients λ for the model relating the K–M($Cr^{3+/2+}$) values and the reaction time and temperature, the gas composition, the support composition and the Cr-loading

Model coefficient λ	Unscaled value
λ_1	0.060
λ_2	0.360
λ_4	-0.015
λ_{44}	$2.203 \cdot 10^{-5}$
λ_{22}	-0.026
λ_0	1.258

K and S, the absorption and scattering coefficients; k, a proportionality coefficient and $C(Cr^{3+/2+})$, the amount of $Cr^{3+/2+}$. However, as was shown in previous publications [3,15,16,22–24], Eq. (3) is only valid for low loaded Cr-catalysts. As a consequence, the K–M($Cr^{2+/3+}$) values will deviate from linearity at higher Cr-loadings. Another important problem is that the scattering coefficient S is support-dependent, and this must be one of the reasons why the intensities will increase with increasing IEP; i.e., with increasing Al_2O_3-content of the support (vide infra). Finally, it is also clear that our analysis does not differentiate between Cr^{2+} and Cr^{3+}, and both are further

referenced as reduced Cr. Therefore, the mathematical model which relate the Cr-speciation with the factors $\mathbf{X}_i$ will only be semi-quantitative.

4.2.2. Development of a mathematical model for describing Cr-speciation

With the same approach as applied for the dehydrogenation activity, it is possible to relate the Cr-speciation to the design factors $\mathbf{X}_i$, namely the reaction time and temperature, the gas composition, the support composition and the Cr-loading. For this response z, a log-transformation was optimal, and the model resulted in an excellent R^2 of 0.95, RMSE of 0.15, and a F-factor. Thus, a statistically significant model was obtained, and the corresponding model coefficients are summarized in Table 4. The quality of the model is visualized in Fig. 6, and shows only a problem with Experiment N20, which corresponds to a 8 wt.% $Cr/SiO_2 \cdot Al_2O_3$ catalyst treated in isobutane at 425°C. This can be due to a higher-order nonlinearity not taken into account in our model. A physicochemical explanation for this higher-order nonlinearity can be found in the fact that for the 8 wt.%
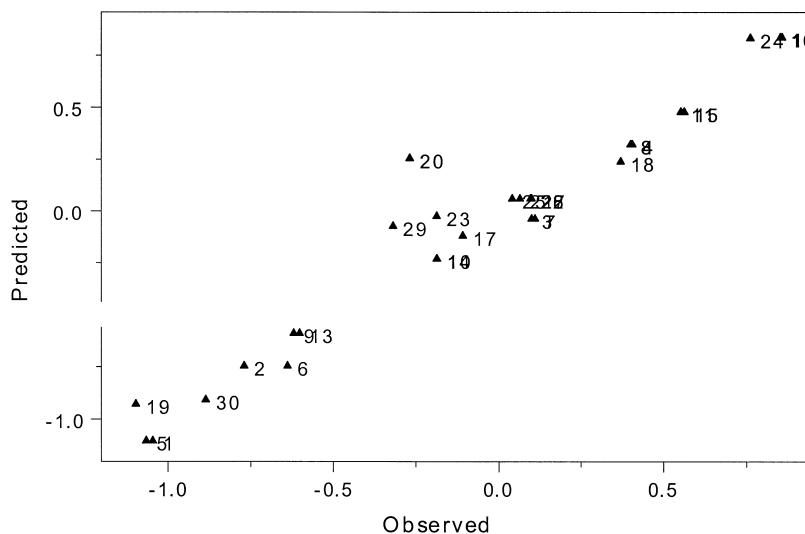

Fig. 6. Predicted vs. observed values of $\log(z)$ for the statistical model relating the K–M ($Cr^{3+/2+}$) values with the factors (model parameters are given in Table 4).
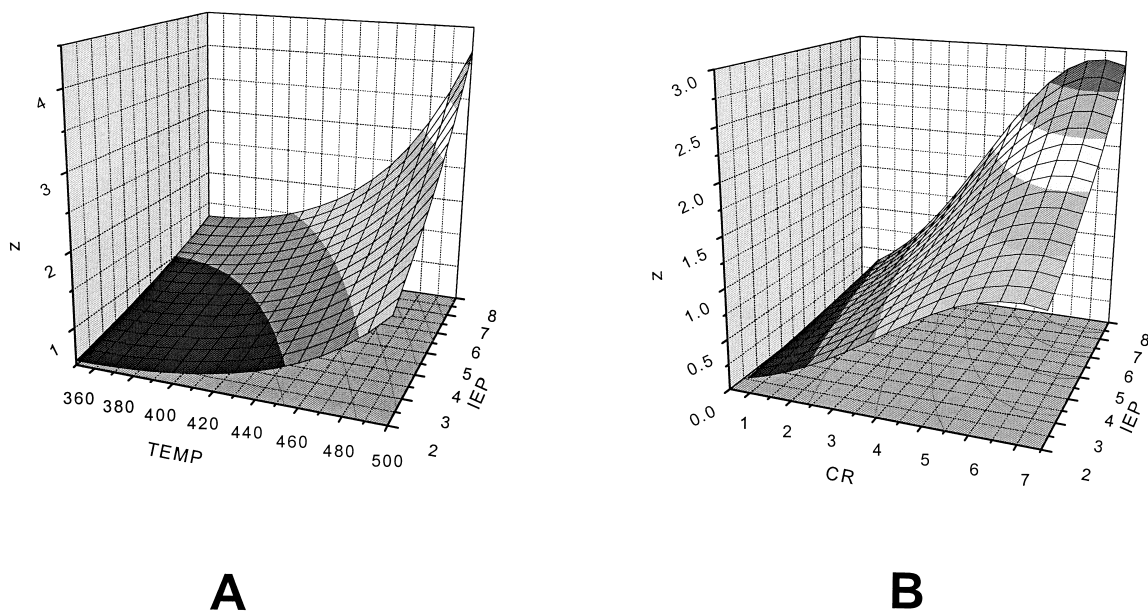
A

B

Fig. 7. (A) Reduced chromium surface plot of the reaction temperature and the IEP (the Cr loading is 4.0 wt.%). (B) Reduced chromium surface plot of the Cr loading and the IEP of the support (the reaction temperature is 425°C).

$Cr/SiO_2 \cdot Al_2O_3$ catalyst monolayer coverage is almost reached resulting in a different surface chemistry.

The relationship between the response z and the different design factors is visualized in Fig. 7. The combined positive influence of the reaction temperature and the IEP on the K–M($Cr^{2+/3+}$) values is visualized in Fig. 7A, but as mentioned before the effect of the IEP of the support is — at least partially — due to the differences in scattering coefficient S between the different supports under investigation. Fig. 7B illustrates the effect of the Cr loading and the IEP of the support on the K–M($Cr^{2+/3+}$) values at 425°C. It is clear that the band intensity increases almost linearly with increasing Cr loading up to a value of about 7 wt.%. The deviation at higher Cr loadings is due to the inherent limitations of the Kubelka–Munk theory [16].

4.3. Quantitative relationship between the Cr-speciation and the catalytic activity

Fig. 8 shows the relationship between the response $y^{1/2}$ and $\log(z)$ over all the experi-

ments of Table 2. This relationship is statistically significant, but definitely not quantitative. The reason is, of course, that the conditions employed for the dehydrogenation catalysts were clearly different (vide supra and Table 2). Therefore, it was decided to built a regression model which relates response y (catalytic activity) to the design factors $\mathbf{X}_i$ giving priority to
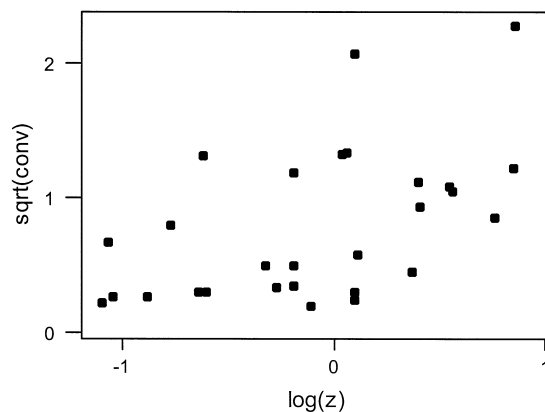

Fig. 8. Quantitative relationship between the catalytic activity ($y^{1/2}$) and the amount of reduced Cr ($\log(z)$) based on the results of Table 2.
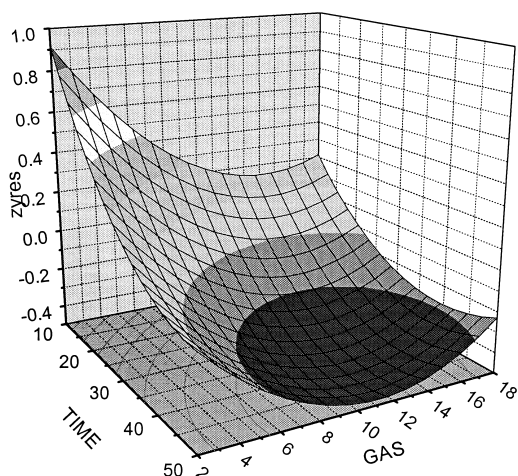
Fig. 9. Response surface plot of the regression model, which relates y to the design factors $\mathbf{X}_3$ (gas composition) and $\mathbf{X}_5$ (reaction time) giving priority to the effect of z.

the effect of response z (K–M($Cr^{2+/3+}$) values). It is important to stress that the variation in response y not explained by response z could be mainly contributed to the factors $\mathbf{X}_3$ (gas composition) and $\mathbf{X}_5$ (reaction time). Fig. 9 visualizes the relationship between the residual of $y^{1/2}$ on log(z) as a function of these two factors. Positive values indicate values where y was higher than predicted by z, negative values indicate y values that were lower than as predicted by z.

Based on the results of Table 2, one can also try to directly relate the catalytic activity with Cr-speciation via linear regression techniques. This is illustrated in Fig. 10 for Cr/Al_2O_3 catalysts, and such analysis is meaningful within one set of dehydrogenation catalysts because both the effect of the scattering coefficient S on the Kubelka–Munk intensity and the differences in Cr-speciation between different amorphous supports are now excluded. It can be concluded — within the limited number of experimental points — that the catalytic activity (response y) is directly proportional with the amount of reduced Cr (response z), and the following equations are obtained:

$$y(\%) = 0.618 z + 0.483 \qquad (4)$$
$$y(\%) = 0.195 z + 0.155 \qquad (5)$$

Eqs. (4) and (5) are obtained for Cr/Al_2O_3 catalysts, which were 10 and 50 min on stream, respectively, and combine the effect of both the Cr loading and the dehydrogenation temperature. The difference in catalytic activity between Cr/Al_2O_3 catalysts, which were 10 or 50 min on stream, must be explained in terms of coking. Thus, the dehydrogenation activity is not only determined by the amount of (pseudo-) octahedral Cr^{3+} — the main species after reduction on an alumina support [3,22–24] — but also by the coking degree, a parameter which was not directly included in the present experimental design.

Table 2 also allows to relate the dehydrogenation activity with the Cr-speciation for 4 wt.% Cr-based catalysts treated under the same conditions, but differing in their support composition, and therefore differing in their redox behavior and diffuse reflectance scattering properties. This is shown in Fig. 11 for experiments N17 (Cr/SiO_2; IEP = 2), N27 ($Cr/SiO_2 \cdot Al_2O_3$-content with 60 wt.% SiO_2; IEP = 5) and N18 (Cr/Al_2O_3; IEP = 8). Fig. 11A relates the response y with the response z for the three 4 wt.% Cr-catalysts treated in isobutane at 425°C for 30 min-on-stream. One can notice that the
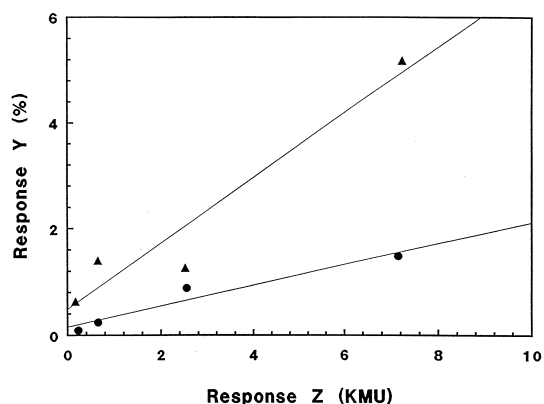

Fig. 10. Quantitative relationship between the catalytic activity (response y) and the amount of reduced Cr (response z) for Cr/Al_2O_3 catalysts as predicted for 10 ($\blacksquare$) and 50 ($\bullet$) min on stream.
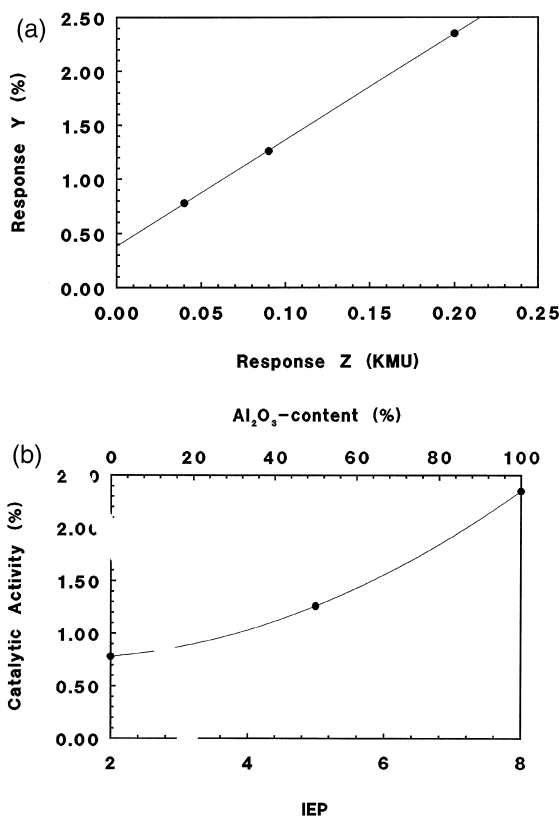
Fig. 11. (A) Quantitative relationship between the catalytic activity (response y) and the amount of reduced Cr (response z) for a 4 wt.% Cr-catalyst at 425°C after 30 min-on-stream for different support compositions or IEPs: Experiment N17 (Cr/SiO_2; IEP = 2), Experiment N27 ($Cr/SiO_2 \cdot Al_2O_3$-content with 60 wt.% SiO_2; IEP = 5) and Experiment N18 (Cr/Al_2O_3; IEP = 8). (B) Dehydrogenation activity as a function of the Al_2O_3-content or IEP of the support (X_2 = 4 wt.%; X_3 = 10% isobutane; X_4 = 425°C and X_5 = 30 min).

catalytic activity almost linearly increases with increasing response z. The same data can also be expressed as a function of the Al_2O_3 content or IEP of the support (Fig. 11B). It is clear that the dehydrogenation activity gradually increases with increasing IEP or Al_2O_3-content of the support. Because the $Cr^{3+}:Cr^{2+}$ ratio on a $SiO_2 \cdot Al_2O_3$ support increases with increasing Al_2O_3-content [3,22–24], it is clear that the dehydrogenation activity gradually increases with increasing $Cr^{3+}:Cr^{2+}$ ratio. In other words,

Cr^{3+}-species are more active for alkane dehydrogenation than Cr^{2+}-species.

5. Discussion

5.1. Evaluation of the method

One of the goals of this work was to explore the possibilities and limitations of an experimental design for the development of quantitative relationships in the field of heterogeneous catalysis. Generally speaking, there were three motivations leading to the use of the present design: (1) performing a minimum of experiments to obtain a maximum of information about the dehydrogenation process; (2) searching for interactions between different parameters or factors. Indeed, interactions between the parameters under study could not be detected by the classical one-variable-at-a-time approach; and (3) developing quantitative relationships which, allows us to make reasonable predictions about the dehydrogenation activity and the Cr-species involved. It is important to stress here that the developed model is based on statistics/mathematics, and cannot be used to operate a catalytic reactor nor to obtain intrinsic reaction constants. Rather, it allows development of (semi-) quantitative relationships which enables us to use DRS as a sensor to follow/optimize catalytic activity and to relate this activity with certain Cr-species. In any case, several well-established mathematical tests were applied in order to guarantee that we have obtained statistical meaningful models, which relates catalytic activity and spectroscopic data with each other.

The performed set of 30 experiments was mainly determined by (1) the factors selected and (2) the chosen borderlines for each of these factors. The former were selected on the basis of literature [1–3] and of preliminary experiments on *n*-butane dehydrogenation [11]. The latter were mainly determined by experimental limitations; i.e., the temperature limitations of the in situ DRS cell, and the problem of satura-

tion in the GC analysis. This is the reason why the application domain of Eq. (2) is rather limited, and that the optimal catalytic conditions were not reached within the present approach. This is clear from Fig. 3, which shows no maximum or optimal dehydrogenation activity. Indeed, the dehydrogenation activity was still increasing with increasing IEP, Cr-loading and reaction temperature, and with decreasing reaction time. Thus, optimal dehydrogenation activity is expected for a high-loaded Cr/Al_2O_3 catalyst working in the temperature range of 550–625°C, and at shorter reaction times. Unfortunately, at the present time no spectroscopic device is available which is able to generate in situ spectroscopic data on both oxidized and reduced Cr-species, and catalytic data to over-span the operational window of an industrial Cr-based dehydrogenation catalyst. The limiting factors are here the very high Cr loadings and reaction temperatures.

By careful examination of the β values of Eq. (2) and Table 3, one can conclude that:
1. There is a positive effect of the Cr loading (X_2) on the dehydrogenation process; and
2. There are positive interactions between the reaction time (X_3) and the gas composition (X_5), and between the support composition (X_1) and the reaction temperature (X_4).

However, presently is it not possible to give a detailed explanation of the model coefficients obtained. Furthermore, the differences between Tables 3 and 4 suggest that solely Cr speciation, as deduced from in situ diffuse reflectance spectroscopy, will not be sufficient to explain all the differences in dehydrogenation activity between Cr-based catalysts. One of the reasons is that the limited number of experiments did not allow to distinguish between the individual contributions of surface Cr^{2+} and Cr^{3+}, which makes an unambiguous determination of the active site for alkane dehydrogenation impossible. In any case, Fig. 11B indicates that Cr^{3+} must be more active than Cr^{2+} explaining the increasing dehydrogenation activity with decreasing SiO_2-content of the support.

5.2. Alkane dehydrogenations and the active Cr species

Eq. (2) allows to calculate the conditions for maximizing the dehydrogenation activity over supported chromium oxide catalysts. The following conditions were obtained: $X_1 = 8$; $X_2 = 7.5$; $X_3 = 2$; $X_4 = 500$ and $X_5 = 10$. Thus, within the limited region of our experimental design, maximum conversion is obtained after 10 min for a 7.5 wt.% Cr/Al_2O_3 catalyst at 500°C with a mixture of 2% isobutane in N_2. The obtained results are in line with literature results, but because our optimum is located at the border of the investigated experimental region, the optimal conditions for isobutane dehydrogenation could not be derived from our model. The optimal dehydrogenation Cr-based catalyst, as determined by careful optimization by catalyst manufacturers over the last decades, is a 13 wt.% Cr/Al_2O_3 catalyst (with some promotors) which operates at 550–625°C, and is regenerated each 10–15 min [1,2]. Summarizing, it is recomforting to see that by applying experimental design in combination with in situ DRS spectroscopy and *on line* GC analysis, conditions close to those used in chemical industries were obtained, confirming the potential of the described approach.

Another comment concerns the catalytic active species for alkane dehydrogenations. The oxidation state of the active Cr-species has been the subject of debate and controversy for many years. According to several authors the active species is Cr^{3+}, while other authors propose both Cr^{2+} and Cr^{3+}, or solely Cr^{2+} as the active species [1]. On the basis of Figs. 10 and 11, one can conclude that: (1) (pseudo-) octahedral Cr^{3+}-ions are actively involved in isobutane dehydrogenation; and (2) Cr^{3+}-species are more active than Cr^{2+}-species.

Finally, it is important to stress that the described methodology could allow to develop an expert system for a dehydrogenation reactor. Such system would allow to predict and control the catalytic activity via direct *on line* spectro-

scopic measurements. Further experiments with a high-temperature optical fiber will be undertaken to substantiate this point.

6. Conclusions

The possibilities and limitations of the use of experimental design in the field of heterogeneous catalysis have been explored by using supported chromium oxide catalysts as an example. A mathematical model, which quantitatively relates catalytic activity and the amount of reduced Cr with the reaction temperature and time, support composition, gas composition and Cr loading, has been developed for the dehydrogenation reaction of isobutane over Cr-based catalysts. This was made possible by combining in situ UV–Vis diffuse reflectance spectroscopy, *on line* GC analysis, and experimental design/chemometrical techniques.

Based on this mathematical model, the following conclusions can be made:
1. the catalytic activity is increasing with increasing Cr loading, dehydrogenation temperature and alumina-content of the support, and with decreasing reaction time and % isobutane in N_2.
2. the dehydrogenation activity is proportional with the amount of in situ measured surface $Cr^{2+/3+}$; Cr^{3+} being more active than Cr^{2+}.
3. the best dehydrogenation catalyst, as proposed by our model, is a 7.5 wt.% Cr/Al_2O_3 catalyst operating at 500°C in 2% isobutane in N_2. This is similar to the industrial catalyst nowadays used in chemical industry.

Acknowledgements

Appendix A. R^2 and Q^2 test

The R^2 and Q^2 test is a technique to evaluate the goodness of fit [25]. R^2 is the percentage of the variation of the response explained by the model, whereas Q^2 is a measure for the predictive power of the model. They are defined as follows: $R^2 = SS_{regr}/SS_{total}$ and $Q^2 = 1 - PRESS/SS_{total}$; with:

$$SS_{total} = \sum_{i=1}^{n} (y_i - \bar{y})^2;$$

$$SS_{regr} = \sum_{i=1}^{n} (\hat{y}_i - \bar{y})^2;$$

$$SS_{res} = \sum_{i=1}^{n} (y_i - \hat{y}_i)^2 \text{ and}$$

$$PRESS = \sum_{i=1}^{n} \frac{(y_i - \hat{y}_i)^2}{(1 - h_i)^2}$$

with h_i = the ith diagonal element of the matrix $X(X^TX)^{-1}X^T$.

Appendix B. ANOVA analysis

The ANOVA is a statistical technique to test the significance of a mathematical model [25]. The ANOVA analysis partitions the total variation of a selected response SS (Sum of Squares corrected for the mean) into a part due to the regression model (SS_{regr}, Sum of Squares explained by the model) and a part due to the residuals (SS_{resid}, Sum of Squares not explained by the model); i.e., $SS = SS_{regr} + SS_{resid}$. For statistical reasons, one has to work with the mean sum of squares (MS): $MS_{regr} = SS_{regr}/D_{f_{regr}}$ and $MS_{res} = SS_{regr}/D_{f_{regr}}$ with D_f, the degree of freedom associated with the variance terms and, the square root of MS is the

standard deviation SD. The zero hypothesis H_0 is then that no model is necessary to describe the experimental results. The ratio MS_{regr}/MS_{res} is characterized by a F-distribution, and the ratio is defined as F. A small F resembles a model with no statistical meaning, whereas a large F is indicative for a statistically meaningful model.

Appendix C. PCA

Principal component analysis (PCA) is a factor analysis method and the model is: $\mathbf{X} = \mathbf{TP}''$ with $\mathbf{X}$ $(n \times p)$, the original data matrix of n samples (spectra) and p variables (wavelengths) [25]. Given a set of p variables, PCA tries to find a set of m variables $\mathbf{T}$ (with $m < p$), in such a way that upon replacement of $\mathbf{X}$ by $\mathbf{T}$ no information is lost. PCA thus results in the transformation of the original x-variables to new t-variables, which are linear combinations of the x-variables. $\mathbf{T}$ $(n \times m)$ is called the scores matrix and $\mathbf{P}$ $(p \times m)$ the loading matrix. The PCA analysis is performed by using the NIPALS algorithm (pcanip) of the Chemometric toolbox of MATLAB.

Appendix D. SIMPLISMA

Simple-to-use self-modeling mixture analysis (SIMPLISMA) is a method to resolve the spectral data matrix $\mathbf{D}$ $(v \times c)$ in pure component spectra [21]. The method is based on the principle of the pure variable. This is a variable, in this case a given wavelength, at which the intensity comes from one chemical component only. The matrix notation is: $\mathbf{D^T} = \mathbf{CS}$, and $\mathbf{D^T}$ $(c \times v)$ contains mixture spectra in its rows. The matrix $\mathbf{C}$ $(c \times n)$ contains in its columns the fractional contributions of the pure components in the mixture spectra, where n is the number of pure components. $\mathbf{S}$ $(n \times v)$ contains the pure spectra. When using in $\mathbf{C}$ the observed intensities of the pure variables in the spectra in $\mathbf{D}$, $\mathbf{S}$ can be resolved by least-squares. The SIMPLISMA software has been developed by Willem Windig and runs under MATLAB.

References

[1] B.M. Weckhuysen, R.A. Schoonheydt, Catal. Today, 1999, 51, 223 and references therein.
[2] F. Buonomo, D. Sanfilippo, F. Trifiro, Handbook of Heterogeneous Catalysis, 1997, 2140 and references therein.
[3] B.M. Weckhuysen, I.E. Wachs, R.A. Schoonheydt, Chem. Rev. 96 (1996) 3327, and references therein.
[4] A. Hakuli, A. Kytokivi, A.O. Krause, T. Suntola, J. Catal. 161 (1996) 393.
[5] F. Cavani, M. Koutyrev, F. Trifiro, A. Bartolini, D. Ghisletti, R. Iezzi, A. Santucci, G. Del Piero, J. Catal. 158 (1996) 236.
[6] H.J. Lugo, J.H. Lunsford, J. Catal. 91 (1985) 155.
[7] A. Kytokovi, J.P. Jacobs, A. Hakuli, J. Merilainen, H.H. Brongersma, J. Catal. 162 (1996) 190.
[8] S. De Rossi, G. Ferraris, S. Fremiotti, E. Garrone, G. Ghiotti, M.C. Campa, V. Indovina, J. Catal. 148 (1994) 36.
[9] B.M. Weckhuysen, I.E. Wachs, J. Phys. Chem. 100 (1996) 14437.
[10] B.M. Weckhuysen, I.E. Wachs, J. Phys. Chem. B 101 (1997) 2793.
[11] B.M. Weckhuysen, A. Bensalem, R.A. Schoonheydt, J. Chem. Soc. Faraday Trans. 94 (1998) 2011.
[12] S. Hellberg, M. Sjostrom, B. Skagerberg, S. Wold, J. Med. Chem. 30 (1987) 1126.
[13] A. Cartier, J.-L. Rivail, Chemom. Intell. Lab. Syst. 1 (1987) 335.
[14] W.J. Dunn, Chemom. Intell. Lab. Syst. 6 (1989) 181.
[15] A. Bensalem, B.M. Weckhuysen, R.A. Schoonheydt, J. Phys. Chem. B 101 (1997) 2824.
[16] B.M. Weckhuysen, R.A. Schoonheydt, Catal. Today 49 (1999) 441.
[17] K.C. Chen, T. Tsuchiya, J.D. Mackenzie, J. Non-Cryst. Solids 81 (1986) 227.
[18] A. Maes, J. Tits, G. Mermans, A. Dierckx, J. Soil Sci. 43 (1992) 669.
[19] B.M. Weckhuysen, A.A. Verberckmoes, A.R. De Baets, R.A. Schoonheydt, J. Catal. 166 (1997) 160.
[20] D.L. Massart, S.N. Vandeginste, Y. De Ming, Y. Michotte, L. Kaufmann, Chemometrics: A Textbook, Elsevier, Amsterdam, 1988.
[21] W. Windig, J. Guilment, Anal. Chem. 63 (1991) 1425.
[22] B.M. Weckhuysen, L.M. De Ridder, R.A. Schoonheydt, J. Phys. Chem. 97 (1993) 4756.
[23] B.M. Weckhuysen, A.A. Verberckmoes, A.L. Buttiens, R.A. Schoonheydt, J. Phys. Chem. 98 (1994) 579.
[24] B.M. Weckhuysen, L.M. De Ridder, P.J. Grobet, R.A. Schoonheydt, J. Phys. Chem. 99 (1995) 320.
[25] Manual Edition of MODDE for windows, graphical software for statistical experimental design, 1995.